Contextual modulation involves suppression and facilitation from the center and the surround

Tim S. Meese   Neurosciences Research Institute, Aston University, Aston Triangle, Birmingham, UK

Robert J. Summers   Neurosciences Research Institute, Aston University, Aston Triangle, Birmingham, UK

David J. Holmes   Neurosciences Research Institute, Aston University, Aston Triangle, Birmingham, UK

Stuart A. Wallis   Neurosciences Research Institute, Aston University, Aston Triangle, Birmingham, UK

In psychophysics, cross-orientation suppression (XOS) and cross-orientation facilitation (XOF) have been measured by investigating mask configuration on the detection threshold of a centrally placed patch of sine-wave grating. Much of the evidence for XOS and XOF comes from studies using low and high spatial frequencies, respectively, where the interactions are thought to arise from within (XOS) and outside (XOF) the footprint of the classical receptive field. We address the relation between these processes here by measuring the effects of various sizes of superimposed and annular cross-oriented masks on detection thresholds at two spatial scales (1 and 7 c/deg) and on contrast increment thresholds at 7 c/deg. A functional model of our results indicates the following (1) XOS and XOF both occur for superimposed and annular masks. (2) XOS declines with spatial frequency but XOF does not. (3) The spatial extent of the interactions does not scale with spatial frequency, meaning that surround-effects are seen primarily at high spatial frequencies. (4) There are two distinct processes involved in XOS: direct divisive suppression and modulation of self-suppression. (5) Whether XOS or XOF wins out depends upon their relative weights and mask contrast. These results prompt enquiry into the effect of spatial frequency at the single-cell level and place new constraints on image-processing models of early visual processing.

Keywords: Human vision, contrast gain control, masking, lateral interactions, model

Introduction

A long-standing view of early vision is that it performs a patch-wise analysis of the retinal image along multiple image dimensions including orientation and spatial frequency (Robson, 1980). The organization of primary visual cortex (V1) is well suited to this task. It contains modules of cells with overlapping receptive fields that are selective for different values along the dimensions of interest (DeValois & DeValois, 1988; Hubel & Wiesel, 1959, 1962; Jones & Palmer, 1987), and because neighboring modules receive input from neighboring regions in the visual field, retinal topography is also preserved (Tootel, Switkes, Silverman, & Hamilton, 1988).

Spatial interactions

Over the last decade or so, much work has focussed on the interactions within and between the filtering modules per-forming local analyses. For example, contrast interactions have been found between neighboring regions on the retina in psychophysics (Ejima & Takahashi, 1985; Ishikawa, Shimegi, & Sato, 2006; Meese & Hess, 2004; Olzak & Laurinen, 1999; Petrov, Carandini, & McKee, 2005; Xing & Heeger, 2000), single-cell physiology (Born & Tootell, 1991; Cavanaugh, Bair, & Movshon, 2002a; Jones, Grieve, Wang, & Sillito, 2001; Levitt & Lund, 1997; Webb, Tinsley, Barraclough, Parker, & Derrington, 2003), and functional imaging (Ohtani, Okamura, Yoshida, Toyama, & Ejima, 2002; Williams, Singh, & Smith, 2003; Zenger-Landolt & Heeger, 2003). Interactions between different spatial frequency and orientation bands at the same location on the retina are also well known (Bonds, 1989; Burr & Morrone, 1987; DeAngelis, Robson, Ohzawa, & Freeman, 1992; Foley, 1994; Meese, 2004; Morrone, Burr, & Maffei, 1982; Ross & Speed, 1991). These studies of contextual modulation are valuable because they open the door to architectural and functional details of the early visual system. In particular, they have implications for contrast gain control (Carandini & Heeger, 1994; Foley,

1994; Levitt & Lund, 1997; Meese, 2004; Tolhurst & Heeger, 1997), image coding strategies (Felsen, Touryan, & Dan, 2005; Guo, Robertson, Mahmoodi, & Young, 2005; Olshausen & Field, 2005; Schwartz & Simoncelli, 2001), contour integration (Field, Hess, & Hayes, 1993; Hess, Dakin, & Field, 1998; Huang, Hess, & Dakin, 2006; Kapadia, Ito, Gilbert, & Westheimer, 1995; Polat & Sagi, 1993; Sillito, Grieve, Jones, Cudeiro, & Davis, 1995), border ownership (Sakai & Nishimura, 2006), and image segmentation (Born & Tootell, 1991; Grigorescu, Petkov, & Westenberg, 2004; Olzak & Laurinen, 2005), although probably not a pop-out phenomena in general (Hegdé & Felleman, 2003; Levitt & Lund, 1997).

Seeing a clear picture across the wealth of studies has been difficult though. This is because different effects have been found for different: field positions (Petrov et al., 2005; Snowden & Hammett, 1998), spatial and temporal frequencies (Meese & Hess, 2004; Meese & Holmes, 2006, 2007; Woods, Nugent, & Peli, 2002), arrangements across eye (Baker, Meese, & Georgeson, in press; Macknik & Martinez-Conde, 2004; Meese & Hess, 2004; Petrov & McKee, 2006), observers (Abbey & Eckstein, 2006; Cannon & Fullenkamp, 1993; Meese, 2004; Meese & Hess, 2004; Meese, Hess, & Williams, 2005; Yu, Klein, & Levi, 2001), levels of practice (Dorais & Sagi, 1997; Kurki, Hyvärinen, & Laurinwn, 2006), levels of attention (Freeman, Driver, Sagi, & Zhaoping, 2003; Shani & Sagi, 2005), stimulus designs (Chen & Tyler, 2002; Yu, Klein, & Levi, 2003), species (Sillito, Cudeiro, & Murphy, 2004; Webb, Dhruv, Solomon, Tailby, & Lennie, 2005; Webb et al., 2002), striate cells (Sillito et al., 1995), and methods of analysis (Cavanaugh et al., 2002a; Cavanaugh, Bair, & Movshon, 2002b; Kapadia et al., 1995). Nevertheless, progress is being made as investigators continue to refine both experiments (Cavanaugh et al., 2002a, 2002b; Li, Thompson, Duong, Peterson, & Freeman, 2006; Petrov & McKee, 2006; Priebe & Ferster, 2006; Smith, Bair, & Movshon, 2006; Webb et al., 2005) and models (Baker & Meese, 2006; Baker, Meese, & Summers, in press; Carandini et al., 2005; Chen & Tyler, 2001; Meese, 2004; Meese & Holmes, 2002; Yu et al., 2003), and the parallels between psychophysics and single-cell work become clearer (see below).

Facilitation and suppression

Modulatory spatial interactions are often allocated to the two categories of facilitation and suppression. Like many other authors, we use these terms here to mean that the visual response (be that of a neuron or a psychophysical mechanism) is either weakened or strengthened by the mask, respectively, but without any direct excitation from the mask.[1]

Single-cell physiology

At the single-cell level of striate cortex, suppression is commonplace for superimposed cross-oriented masks (e.g., Bonds, 1989; DeAngelis et al., 1992; Morrone et al., 1982). ('Cross-oriented' masks are those at an orientation sub-

stantially different from the test, but not necessarily orthogonal to it.) Surrounding masks (annuli) or flankers (pairs of patches) whose orientations are the same as the test (sometimes called co-oriented or parallel) can also have a strong suppressive influence (Bair, Cavanaugh, & Movshon, 2003; Born & Tootell, 1991; Hubel & Wiesel, 1962; Jones et al., 2001; Levitt & Lund, 1997; Sillito et al., 1995). And suppression has also been found for cross-oriented masks in the surround although the effects are weaker than in the co-oriented case and become still less potent as the central test contrast increases (Cavanaugh et al., 2002b; Levitt & Lund, 1997; Webb et al., 2005). Some of these suppressive effects probably involve inhibitory interactions within the cortex (Bair et al., 2003; Heeger, 1992; Morrone, Burr, & Speed, 1987; Sengpiel & Vorobyov, 2005; Webb et al., 2005), whereas others have been attributed to the lateral geniculate nucleus (Baker, Meese, & Summers, in press; Bonin, Mante, & Carandini, 2005; Li et al., 2006; Ozeki et al., 2004; Priebe & Ferster, 2006; Smith et al., 2006; Solomon, White, & Martin, 2002) and depression within the thalamocortical synapse (Freeman, Durand, Kiper, & Carandini, 2002).

By comparison, facilitatory modulation is not so widespread. Early single-cell work reported that co-oriented stimuli in the surround could produce facilitation (Kapadia et al., 1995; Nelson & Frost, 1985), but it has been suggested that this was due to direct subthreshold excitation of the central mechanism by the mask (Cavanaugh et al., 2002a). If so, then facilitatory interactions from the surround are possibly restricted to the cross-oriented case (Cavanaugh et al., 2002b; Jones et al., 2001; Jones, Wang, & Sillito, 2002; Levitt & Lund, 1997; Sillito & Jones, 1996). Such interactions might involve direct influences on the contrast gain or an intermediate process of disinhibition (Cavanaugh et al., 2002b; Sillito et al., 1995).

Psychophysics

There are some strong parallels between the cellular results above and the results from psychophysics. First, suppression has been inferred for the same three situations as for individual neurons. That is, (1) superimposed cross-oriented masks reduce perceived contrast (Meese & Hess, 2004) and raise detection thresholds (Foley, 1994). (2) High contrast co-oriented surrounds reduce perceived contrast in the periphery (Xing & Heeger, 2000) and in the fovea (Cannon & Fullenkamp, 1991) and raise detection thresholds in the periphery (Petrov et al., 2005; Snowden & Hammett, 1998). (3) Cross-oriented masks in the surround reduce perceived contrast (Meese & Hess, 2004; Solomon, Sperling, & Chubb, 1993; Xing & Heeger, 2001), although the effects are weaker than for the co-oriented case (Ishikawa et al., 2006; Solomon et al., 1993).

As in the single-cell work, interpretation of psychophysical facilitatory interactions is less clear. Early evidence suggested facilitation from co-axial flankers in a co-oriented configuration (Chen & Tyler, 2001; Kapadia et al., 1995; Polat & Sagi, 1993), but later work found that similarly placed cross-oriented flankers (Chen & Tyler, 2002) or cross-

oriented surrounds (Meese & Hess, 2004; Yu, Klein, & Levi, 2002; Yu et al., 2003) could achieve the same effects, as well as enhancing perceived contrast of suprathreshold targets (Xing & Heeger, 2001; Yu et al., 2001). In fact, the co-oriented case has been criticized on similar grounds to the single-cell work above (Solomon, Watson, & Morgan, 1999), although a complete understanding probably involves a more elaborate scheme than originally proposed (Huang et al., 2006; Solomon & Morgan, 2000). In any case, the directly observable effect of facilitation from co-axial and co-oriented flankers is fragile because it is diminished when other co-oriented (Polat, 1999; Solomon & Morgan, 2000) or cross-oriented (Kapadia et al., 1995) stimuli are placed in the spatial vicinity. Another possibility is that co-oriented flankers enhance the observer's overall signal-to-noise ratio by reducing uncertainty (Petrov, Verghese, & McKee, 2006; Williams & Hess, 1998; Woods et al., 2002; Yu et al., 2002). Such a process would have no obvious counterpart at the single-cell level and would be strictly a threshold phenomenon because pedestals (i.e., masks that raise the contrast against which test increments are judged) provide their own reduction of uncertainty (Pelli, 1985; Yu et al., 2002). However, it is likely that other processes are at least associated with facilitation because lateral flankers elongate the classification image used in the detection process (Kurki et al., 2006).

Detection of a target on a pedestal (sometimes referred to as contrast discrimination) has also been used to investigate contextual interactions. Several studies have observed effects of co-oriented (Foley, 1994; Foley & Chen, 1997; Meese, 2004) and cross-oriented (Yu & Levi, 2000; Yu et al., 2002, 2003) surrounds on detection of central contrast increments of a pedestal. This approach provides a good test of the generality of models of cross-orientation interactions (XOI) (see our Experiment 2) because it pushes the target mechanism into its supra-threshold operating characteristic. However, it does not provide a direct test of the category of modulation because in some situations, a single category [cross-orientation facilitation (XOF) or cross-orientation suppression (XOS)] can either enhance or degrade performance, depending upon stimulus details and model parameters (Meese, 2004; Meese et al., 2005). This is because contrast discrimination does not relate to the magnitude, but the first derivative of the contrast response, and so the effect of masking can be counterintuitive (Bruce, Green, & Georgeson, 2003; Meese, 2004). Consequently, the results of this type of experiment relate to the single-cell work much less directly and require detailed quantitative modelling for safe interpretation.

Motivation, aims, and outcomes

In the present work, we confine our interests to cross-oriented interactions (XOI), for which there is less controversy. The review above presents a coherent picture in which (i) XOS is produced by masks placed in the center and in some cases the surround, and (ii) XOF is produced by masks placed in the surround.

The original motivation for the present work stemmed from the apparently conflicting findings of Yu et al. (2002) and Meese (2004) regarding influences from the surround. In the first of these studies, evidence was presented for sensory facilitation by cross-oriented annular masks. In the second study, it was found that extending the size of a superimposed cross-oriented mask had no effect. In other words, Yu et al. (2002) found interactions from a cross-oriented surround whereas Meese (2004) did not. To investigate this, we performed experiments using similar stimulus configurations (annular masks and small and large superimposed masks) and spatial frequencies (low and high spatial frequencies) as in each of the two previous studies. Thus, we began by asking what happens to XOF from the surround when an annular mask is extended to fill the central hole. But from this a much broader set of questions emerged, including the following: What determines whether facilitation or suppression wins out in the surround? Is XOF restricted to the surround? Does XOF occur at low spatial frequencies? Is there one or more forms of XOS? Can a single functional model be devised to describe XOI both at and above detection threshold, for a wide range of spatial frequencies and mask configurations?

We perform two psychophysical experiments to address these questions and more generally to characterize the interplay between XOS and XOF. We develop a quantitative model of the results at detection threshold, which shows that the weight of XOS but not XOF declines with spatial frequency, and that the drives for both of these interactions are evident in the central mask region. At low spatial frequencies (1 c/deg), the drives become very weak in the surround, but at high spatial frequencies (7 c/deg) they remain similar to those in the center. This is consistent with a model in which the region for XOI is determined by a fixed retinal angle rather than a fixed number of target cycles. The details of the model are refined in a second experiment in which a combination of pedestal and cross-oriented masks is used. The results suggest that there are two sources of XOS from both center and surround. One involves direct divisive suppression of the detecting mechanism, and the other involves modulation of self-suppression.

Methods

Observers

Five undergraduate optometry students (RS, BX, LM, RL, and KS) performed the experiment as part of their course requirement. Two of the authors (DJH and RJS) and a postgraduate volunteer (DHB) also served as observers. All observers had substantial practice in all the stimulus conditions before data collection began and had normal or optically corrected to normal vision. Each observer performed all five spatial configurations for a single stimulus condition

only in Experiment 1. Experiment 2 was performed by RJS, DHB, and DJH only.

Equipment

The experiments were run under the control of a PC, and stimuli were displayed from a framestore of a VSG2/4 operating in pseudo-15 bit mode on a 120-Hz grey scale monitor [an Eizo F553-M (mean luminance of 50 cd/m^2)]. Contrast is expressed in dB re 1%, given by $20 \log_{10}(c)$, where c is the Michelson contrast in percent given by $c = 100(L_{max} - L_{min}) / (L_{max} + L_{min})$, L is the luminance. (So, for example, -6 dB = 0.5%, 0 dB = 1%; 6 dB = 2%, 12 dB = 4%, and so on). Mean luminance was constant throughout the experiments.

Gamma correction used lookup tables and ensured that the monitor was linear over the entire luminance range used in the experiments. A frame interleaving technique was used for test and mask stimuli, giving a picture refresh rate of 60 Hz. Observers were seated in a darkened room and sat with their heads in a chin and head rest at a viewing distance of 114 cm. Viewing was always binocular and stimuli were always presented in the center of the display. A small dark fixation point or points were visible throughout the experiment. For the low spatial frequency test stimuli (1 c/deg), this was a single point placed in the center of the display. For the high spatial frequency test stimuli (7 c/deg), this was a square arrangement of four points, each placed 0.62° from the center of the display. This placed them just inside the skirts of the large masks.

For the highest spatial frequency that we used (7 c/deg), there were 10 pixels per cycle. Space averaged luminance measurements of vertical and horizontal sine-wave gratings over a range of contrasts at this spatial frequency confirmed that there was no reduction in luminance due to adjacent pixel nonlinearity for our stimuli (García-Pérez & Peli, 2001; Woods et al., 2002).

Stimuli for Experiment 1

In Experiment 1 there were three main stimulus conditions, each with five spatial configurations and a further two configurations for one of these conditions (i.e., 17 stimuli in total). These were as follows.

Orthogonal 1 c/deg condition

The test stimulus was always a horizontal, sine-phase, 1 c/deg sine-wave grating, modulated by a raised-sine function with a one-cycle rise, a one-cycle fall, and a central plateau of one cycle. Thus, the full diameter of the test stimulus was 3 cycles and the full width at half height of the envelope was 2 cycles (Figure 1A). The mask was always a vertical, sine-phase, 1 c/deg grating and was modulated by one of five different mask envelopes. These were small, medium, and large patches and medium and large
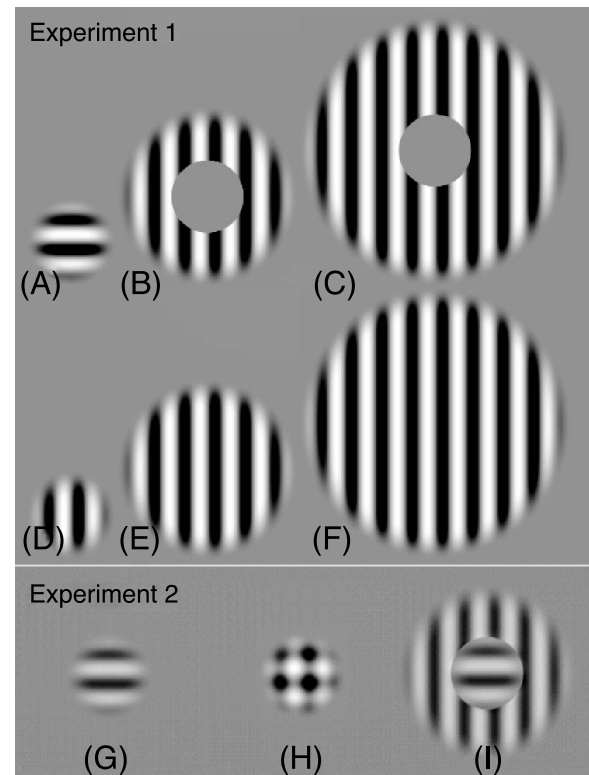

Figure 1. High contrast examples of stimuli used in the experiments. Top panel (Experiment 1): (A) Test stimulus. (B, C) Medium and large doughnut masks. (D–F) Small, medium, and large superimposed masks. The diameters of the holes in B and C are the same. The contrasts of the masks (B–F) varied in the range 0% to 45%. Bottom panel (Experiment 2): (G) Test and pedestal (the same as panel A). (H) Pedestal plus small, superimposed mask (the sum of panels A and D). (I) Pedestal plus medium doughnut mask (the sum of panels A and B). The mask was either 0% or 10% and the contrast of the pedestal varied in the range 0% to 32%.

doughnuts (annuli). The spatial envelope of the small patch mask was identical to that of the test stimulus. For the medium patch, the central plateau was 4° (4 cycles) and for the large patch the central plateau was 7° (7 cycles). The rise and fall of the raised cosine function at the blurred outer boundary was the same as that for the target patch (1°, 1 cycle). The medium and large annuli had the same outer diameters and blurred boundaries as the medium and large patches, but both had a central hole, 2.4° in diameter and blurred by a raised sine function 2 pixels in width, to achieve anti-aliasing. The diameter of the hole was equivalent to 2.4 cycles of the test stimulus and matches that used by Yu and Levi (2000). The five mask stimuli are shown in Figures 1B–F.

Mixed condition

The test stimulus was identical to that in the orthogonal 1 c/deg condition. The mask stimuli had the same spatial envelopes as those in the orthogonal 1 c/deg condition, but

the carrier was a right oblique (45°), 3 c/deg grating (Holmes & Meese, 2004; Meese, 2004; Meese & Hess, 2004; Meese & Holmes, 2002).

Orthogonal 7 c/deg condition

This was identical to the orthogonal 1 c/deg condition except that all the spatial dimensions were scaled by a factor of seven. Thus, the mask and test stimuli had a spatial frequency of 7 c/deg and were one-seventh the diameters of those in the orthogonal 1 c/deg condition. The one exception to this scaling was the blurring of the holes in the annuli, which remained at 2 pixels.

Very large orthogonal 7 c/deg condition

In a final arrangement, the orthogonal 7 c/deg condition was repeated, with the single change that the outer diameter of the spatial envelope of the large patch and annulus were extended to match those in the orthogonal 1 c/deg condition (8° full-width at half-height). Here, we refer to this as a 'very large' mask.

Pedestal experiment (Experiment 2)

In Experiment 2, the small stimulus patch (Figure 1G) was used as both a test stimulus and a pedestal (a pedestal is a mask that is spatially matched to the test). The test was detected in the presence of the pedestal plus a mask with a fixed contrast of either 0% or 10%. In a superimposed configuration, the mask was the small orthogonal patch (Figure 1H). In a doughnut configuration, the mask was the medium annulus (Figure 1I). The spatial frequency of test, pedestal, and mask was 7 c/deg. DJH and RJS performed the two mask-contrast conditions for the superimposed configuration before the doughnut configuration. Thus, they performed the experiment with a pedestal and 0% fixed mask condition twice. DHB performed the two configurations in randomized blocks and performed the four replications of each configuration only once.

Abbreviations

For brevity, we denote the various spatial configurations using two characters. The first refers to whether the mask was superimposed (S) or a doughnut (D). The second refers to the size of the mask, which could be small (S), medium (M), large (L), or very large (V).

Procedure

Test contrast level was selected by a three-down one-up staircase procedure (Wetherill & Levitt, 1965) and a single condition was tested using a pair of randomly interleaved staircases (Cornsweet, 1962). After an initial experimental stage in which larger step-sizes were used (8 dB and 4 dB),

a test stage consisted of 12 reversals for each staircase using a contrast step-size of 2 dB. A two-interval forced-choice (2 IFC) technique was used, where one interval (the null interval) contained only the mask and the other (the test interval) contained the test plus mask. (Thus, the test and mask (see Figure 1) overlapped exactly in both space and time.) The onset of each 200 ms test interval was indicated by an auditory tone and the duration between the two intervals was 400 ms. The observer's task was to select the test interval using one of two buttons to indicate their response. Correctness of response was provided by auditory feedback, and the order of the intervals was selected randomly by the computer. For each run, thresholds (75% correct) and standard errors were estimated by performing probit analysis on the data gathered during the test stages of the testing procedure (above) and collapsed across the two staircases. This resulted in individual estimates for each psychometric function based on around 100 trials.

In Experiment 1 experimental 'contrast-blocs' were repeated four times. A contrast-bloc consisted of a set of 'mini-blocs' for each of 7 or 11 mask contrasts (including 0%). Observers were instructed to select the mask contrasts in a random order, but to try and spread their selections evenly across the range. A mini-bloc consisted of an experimental session for each of the five mask configurations (three circular patch sizes and two annulus sizes; see Figure 1), performed in a random order determined by a random number generator. The procedure for Experiment 2 was similar, but the 'mini-blocs' consisted of the two different mask contrast conditions (0% and 10%). Pedestal contrast was varied across sessions and the superimposed configuration was tested before the surround configuration.

Before data collection began (and consistent with much of our earlier work), the following rejection and replacement criterion was set to lessen the impact of unreliable estimates of threshold. If the standard error of a threshold estimate within a mini-bloc was greater than 3 dB (estimated by probit analysis), the data for that condition were discarded and the mini-bloc was rerun. Estimates of threshold were averaged across all the replications giving results based on around 400 trials per data point. The exception to this was the estimate of baseline in Experiment 1 (a 'no mask' condition in which mask contrast was 0%). This mask level was included in each of the five mask configurations, meaning that for each stimulus condition an overall estimate was available from 20 replications, about 2000 trials. This produced very reliable estimates of the baseline, as shown by the small error bars for those conditions.

Appearance of stimuli in null and test intervals

During the experiments, the test stimulus was driven very close to detection or discrimination threshold by the staircase procedure. Thus, on a typical 2IFC trial in Experiment 1, the stimulus in the test interval looked like the mask (e.g., Figures 1B–F), but with barely visible hori-

zontal stripes (Figure 1A) superimposed across the center. The stimulus in the null interval was the mask alone. In Experiment 2, the stimulus was that in Figures 1G–I and the task was always to detect contrast increments of the central horizontal patch. Thus, the stimulus had the same spatial appearance in the null and test intervals, but the horizontal patch had slightly higher contrast in the test interval.

Results: Masking functions at detection threshold (Experiment 1)

Low test spatial frequency (orthogonal and mixed conditions)

The results for the 1 c/deg test conditions are shown in Figure 2. Regardless of whether the mask was an orthogonal 1 c/deg grating (top row) or an oblique 3 c/deg grating (bottom row), the pattern of results was very similar. For the superimposed configurations (S*), masking (threshold elevation) increased with mask contrast once the mask was greater than a few percent (~6 dB or 2%). In some cases, this was quite substantial [e.g., >15 dB (a factor of 5.6) for observer BX]. The level of masking was very similar for all three sizes of mask (SS, SM, and SL; blue symbols), indicating little or no extra influence from the surround over that from the small, superimposed mask. This confirms the findings of Meese (2004).

For the doughnut (annular) masks (DM and DL; red symbols), there are small amounts of XOF (≤3 dB) at intermediate mask contrasts, although the effect is more marked for some observers (e.g., BX) than for others (e.g., LM). This extends Yu et al.'s (2002) result to the lower test spatial frequency used here (1 c/deg).
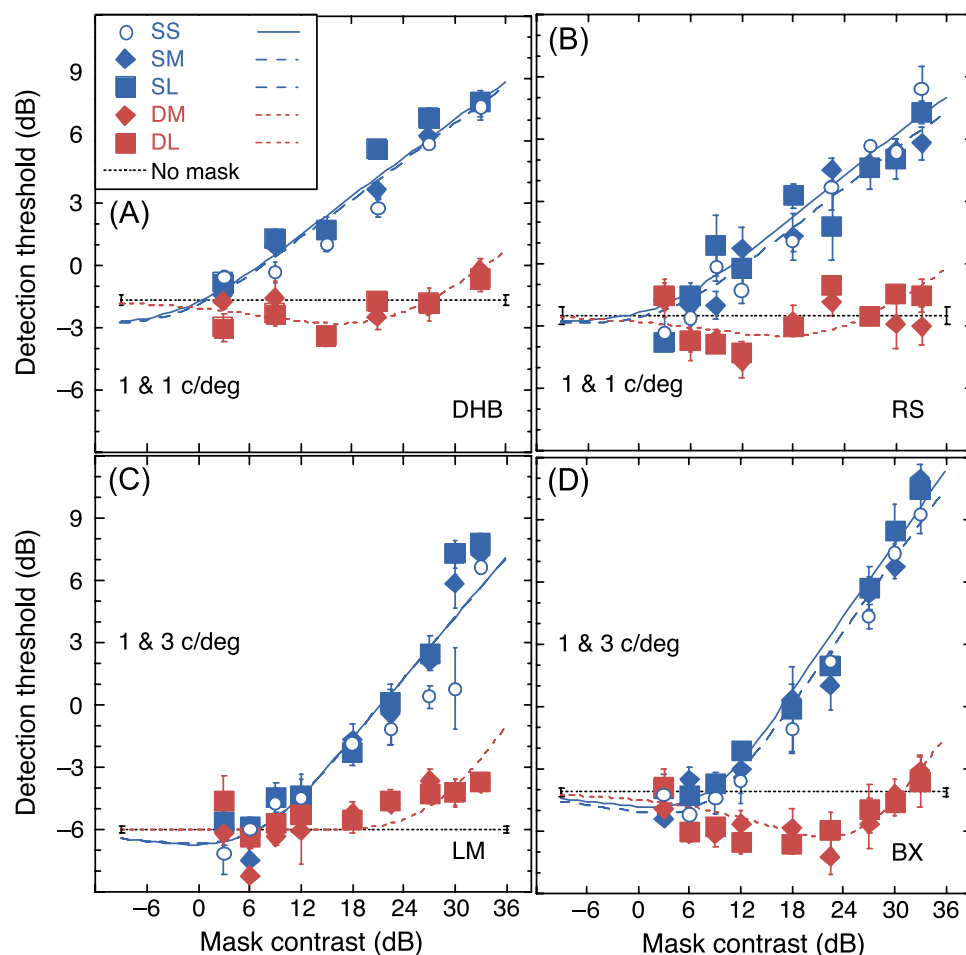

Figure 2. Results for the conditions in which the test stimulus had a spatial frequency of 1 c/deg. Different panels are for different observers. In the top row the mask had a spatial frequency of 1 c/deg and was oriented at right angles to the horizontal target (orthogonal 1 c/deg condition). In the bottom row, the mask had a spatial frequency of 3 c/deg and oblique orientation (45°) (mixed condition). Different symbols denote different spatial configurations. Test and mask were either superimposed (S*) or in an annular (doughnut) configuration (D*). The outer diameter of the mask was small (*S), medium (*M), or large (*L). The horizontal dashed line indicates detection threshold in the absence of a mask. Each data point is estimated from ~400 trials. The baseline is estimated from ~2000 trials. Error bars show ±1 SE. The curves are for the model fits described in the text.

At higher mask contrasts facilitation gives way to masking, although it is never as severe as it is for the superimposed case, and for some observers (BX and RS) it is barely noticeable. Yu et al.'s (2002) observers also showed a decline of facilitation at higher surround mask contrast, but their functions never crossed back over the baseline.

Like in the superimposed case, it is clear from Figure 2 that the size of the annular surround (conditions DM verses DL) has little or no affect on the shape of the masking functions.

Figure 2 also shows that the effects of (i) XOS from the center and (ii) XOF from the surround do not combine linearly. If they did then the masking functions for the two larger superimposed configurations (filled blue symbols) should fall below those from the small, superimposed configuration (open blue symbols) at the mask contrasts for which the doughnut produced facilitation. Clearly they do not. Other types of nonlinear interaction of contextual modulation have been found before (Polat, 1999; Solomon & Morgan, 2000).

High test spatial frequency

At 7 c/deg, the pattern of results was very different from that at the lower test spatial frequency (compare Figure 3 with Figure 2; note that the ordinate has the same scale). XOF was evident for all four observers over much of the contrast range tested, beginning at a mask contrast close to the detection threshold of the target. For the annular masks (red symbols), this is very similar to the results of Yu et al. (2002). But the result with the superimposed mask (blue symbols) is novel and surprising. The facilitation from the superimposed mask has a very similar character to that from the surround mask, suggesting a similar cause.

For the observers in Figures 3C and D, the large stimulus was replaced by a 'very large' stimulus (the diameter was increased by a factor of 7). This was to test an idea that the facilitation might be due to the proximity of the boundary of the mask and the test patch (Meese, 2004). (This was a possibility for all of the configurations used in the top row of Figure 3, where the mask boundary was al-
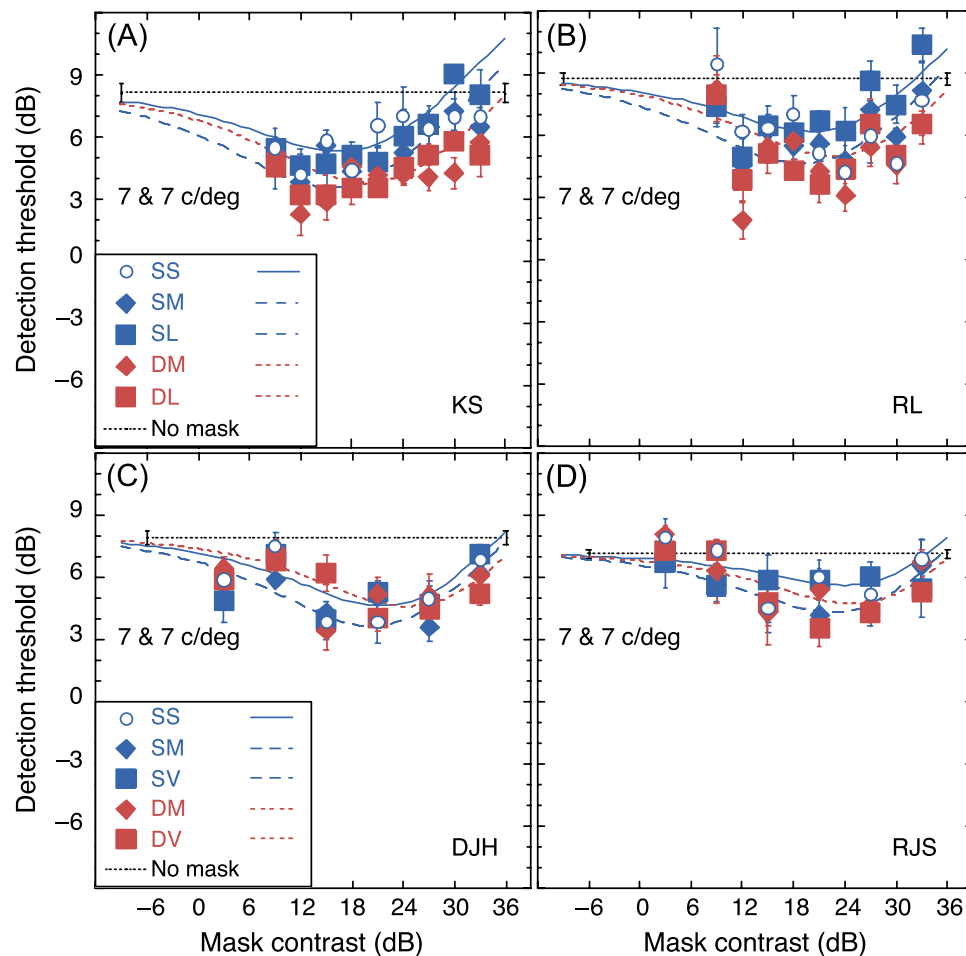

Figure 3. Results for the conditions in which the test and mask stimuli had a spatial frequency of 7 c/deg. Different panels are for different observers. Different symbols denote different spatial configurations. Test and mask were either superimposed (S*) or in an annular (doughnut) configuration (D*). In the top row the outer diameter of the mask was small (*S), medium (*M), or large (*L). In the bottom row it was either small (*S), medium (*M), or very large (*V). The horizontal dashed line indicates detection threshold in the absence of a mask. Each data point is estimated from ~400 trials. The baseline is estimated from ~2000 trials. Error bars show ±1 SE. The curves are for the model fits described in the text.

ways within 0.6° of visual arc of the test patch.) For RJS, the superimposed very large mask did produce slightly lower levels of facilitation than the medium mask, but this reduction was not evident for DJH (compare solid blue squares and diamonds within Figures 3C and D). Thus, it is clear that facilitation cannot be attributed to the nearness of a (mask) boundary contour.

Divisive suppression model for XOI (Model 1)

To better understand the details of the cross-orientation interactions (XOI) that we have measured, we developed a quantitative model of the data. The class of model that we consider is sometimes called a functional model because it takes a parameter list of the stimulus as input (e.g., mask type, mask contrast, and so forth) and transforms this to a decision variable using a mathematical function (or functions) to predict the test contrast required for detection or discrimination threshold. Although not expressed in terms of neural elements, this class of model is valuable because it can provide the systems design for more complete image-processing models (e.g., Watson & Solomon, 1997).

The first model that we tested was an extension of one used in a parallel study by Meese and Holmes (2007) (discussed further below) and has some similarities with the contrast gain control equations used by Heeger (1992) and others. The response of the detecting mechanism in the Meese and Holmes (2007) study is given by:

$$\text{resp} = \frac{c_{\text{test}}^p(1 + \alpha c_{\text{xcenter}})}{z + c_{\text{test}}^q + w c_{\text{xcenter}}^q},\tag{1}$$

where c_{test} and c_{xcenter} are test and superimposed, cross-oriented mask contrasts (in %), and p, q, α, and w are free parameters. The exponents p and q describe the rate of acceleration of nonlinear contrast responses on the numerator and denominator of the gain control equation, respectively. These parameters were not very well constrained by the data from the experiments here. For the 1 c/deg conditions, where masking was strong and provided some constraint, we allowed q to be free, and set $p = q + 0.4$, broadly consistent with numerous observations from pedestal masking studies. For the 7 c/deg conditions, we set $p = 2.0$ and $q = 2.4$, also consistent with other work (e.g., Legge & Foley, 1980).

When the c_{test} term is zero, the saturation constant z does not represent a degree of freedom. As the c_{test} term is negligible for the low test contrast conditions here, z was set to unity.

The parameters α and w are the weights of modulatory facilitation and divisive suppression from the mask. But as these can originate from both center and surround in the present study, Equation 1 needs to be extended to accommodate this. From the data we observed little or no systematic difference between the medium surround conditions (*M) and any of the larger surround conditions (*L & *V), and so we treat all of the surround conditions together in

the modelling. To do this, we consider a simple additive arrangement of center and surround terms as follows:

$$\text{resp} = \frac{c_{\text{test}}^p(1 + \alpha_{\text{center}} c_{\text{xcenter}} + \alpha_{\text{surround}} c_{\text{xsurround}})}{z + c_{\text{test}}^q + w_{\text{center}} c_{\text{xcenter}}^q + w_{\text{surround}} c_{\text{xsurround}}^q}.\tag{2}$$

In 2 IFC, the decision variable at threshold is given by the difference between the detecting mechanism's response to the mask alone, and the mask plus test:

$$\text{resp}_{\text{mask + test}} - \text{resp}_{\text{mask}} = k.\tag{3}$$

Several interpretations of k are possible, but a convenient one is that it is proportional to the standard deviation of late additive noise in the model. When k is a free parameter, it controls the observer's overall sensitivity (i.e., the vertical position of the masking functions on a log plot). However, our estimates of baseline were based on substantially more data than the thresholds at other mask contrasts, so we constrained the model to intercept the 'no-mask' detection threshold in each masking function. We did this by normalizing all of the detection thresholds to the baseline which, from Equations 2 and 3, constrains $k = 0.5$. Model and data were then de-normalized by the original baseline data before plotting. Thus, for each observer the fitting involved four free parameters for the 7 c/deg conditions (α_{center}, α_{surround}, w_{center}, w_{surround}) and five free parameters for the 1 c/deg conditions (where the extra parameter was q).

Fitting was achieved using a downhill simplex algorithm to minimize the square of the differences of the logarithm of model and data. Formally, the RMS error is expressed (in dB) as follows: $\text{RMS}_{\text{error}} = \frac{1}{n}\sum_{i=1:n}\left[20\log_{10}\left(x_i/\hat{x}_i\right)\right]^2$, where x_i and $\hat{x}_i$ are the data and model predictions, respectively (test contrasts in %), for the ith of n data points. The model equation was solved numerically for c_{test} to produce three curves for five masking functions fitted simultaneously to the data ($n = 5\times$ number of mask contrasts in each function, excluding 0%).

The fits are shown by the curves in Figures 2 and 3 and are very good. Best fit parameter values, RMS errors, and other details are shown in Table 1. RMS errors are typically in the order of 1 dB and are never worse than 1.5 dB.

Weight of suppression and facilitation in center and surround

A more informative view of the weight parameters from the fitting of Model 1 in Experiment 1 (Table 1) is offered in Figure 4, where they have been averaged (geometric means) for the 1 and 7 c/deg conditions. Comparisons across the two test spatial frequencies (1 and 7 c/deg) are problematic because of the different contrast sensitivities. To combat this, we first adjusted the model weights by the scaling factor shown in the last column of Table 1, which

Condition (test and mask, c/deg)	Observer	RMS error (dB)	p (fixed)	q (free and fixed)	α_{center} (free)	$\alpha_{surround}$ (free)	w_{center} (free)	$w_{surround}$ (free)	Baseline (no-mask detection threshold, dB)	Parameter scaling factor (Figure 4)
1 and 1	DHB	0.7	$q + 0.4$	1.56	0.588	0.049	1.2488	0.0165	−1.713	0.82
1 and 1	RS	1.00	$q + 0.4$	1.56	0.268	0.061	0.5861	0.0212	−2.48	0.75
1 and 3	LM	1.20	$q + 0.4$	2.16	0.251	0.005	0.1978	0.0008	−5.99	0.50
1 and 3	BX	0.91	$q + 0.4$	2.77	0.200	0.080	0.0786	0.0003	−4.14	0.62
7 and 7	RL	1.50	2.4	2.0	0.112	0.147	0.0054	0.0039	8.71	2.73
7 and 7	KS	1.13	2.4	2.0	0.193	0.258	0.0131	0.0078	8.07	2.53
7 and 7	DJH	0.95	2.4	2.0	0.137	0.099	0.0046	0.0023	7.89	2.48
7 and 7	RJS	0.84	2.4	2.0	0.038	0.061	0.0015	0.0018	7.13	2.27

Table 1. Parameter values and other details for the fits of the divisive suppression model (Model 1) (Equations 2 and 3) to the results from Experiment 1. The exponent q was a free parameter for the fits to the 1 c/deg condition (top four rows) but fixed at $q = 2.0$ for the 7 c/deg conditions (bottom four rows). The 'parameter scaling factor' (final column) was used in producing Figure 4 and is the baseline detection threshold in percent.

is the baseline detection threshold in percent. Essentially, this normalizes the mask contrast to the detection threshold for the test stimulus and has the effect of increasing the weights in the 7 c/deg conditions relative to those in the 1 c/deg conditions. (In the absence of detection thresholds for the masks, this provides a rough approximation to what is required.) Note that this normalization procedure leaves the relative weights within each of the spatial frequency conditions untouched. Finally, the weights were all plotted relative to the facilitatory weight for the 1 c/deg center in Figure 4.

Consider the center weights first (left part of Figure 4). The facilitatory weight (α) is fairly unaffected by spatial frequency (compare the two green circles), but the suppressive weight is much lower at the higher spatial frequency (compare the two red squares). This is why masking is seen
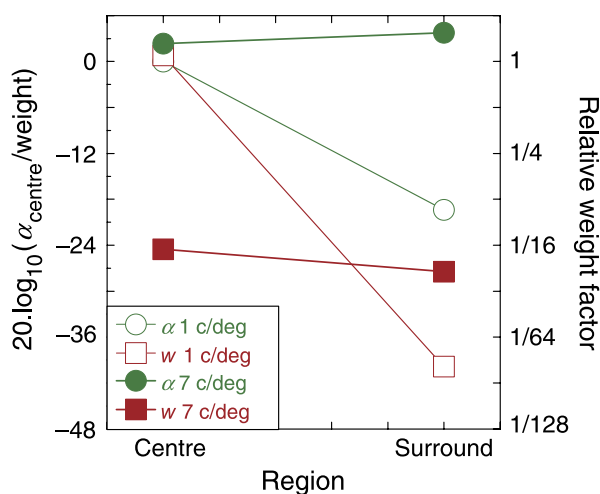

Figure 4. Summary of facilitatory weights (circles) and suppressive weights (squares) for the divisive suppression model (Model 1) fitted to the results from Experiment 1. The open symbols are for the 1 c/deg test conditions and the solid symbols are for the 7 c/deg condition.

primarily at the low spatial frequency. Now consider how the weights change across mask region. At 7 c/deg, the weights are very similar for the center and the surround (the solid symbols are connected by almost parallel lines), and suppression is relatively weak. This is why the masking functions in Figure 3 (7 c/deg) are all very similar, and dominated by facilitation. In contrast, at 1 c/deg both weights are relatively high in the center, but decline substantially in the surround (the open symbols are connected by lines with negative slope), more so for suppression than facilitation. This is why masking dominates in the center in Figure 2 (1 c/deg), but facilitation becomes apparent when the mask is restricted to the surround.

In sum, the analysis shows that XOI is not scale-invariant in terms of either (i) the effects from the center (they are different at 1 and 7 c/deg) or (ii) their spatial extent (the interactions extend over a greater number of cycles, at 7 c/deg).

This result has a striking parallel with the co-oriented suppressive interactions found by Petrov and McKee (2006) who measured contrast detection in the periphery. They found that surround suppression was greater at the lower spatial frequency that they tested (1.3 c/deg verses 2.6 c/deg) and that the spatial extent of suppression did not scale with spatial frequency but was of a constant retinal angle. It is possible that a similar spatial arrangement underlies the XOI measured here. Further experiments would be required to establish this but might be problematic given the small size of the effects (~3 dB).

Results: Pedestal masking (Experiment 2)

Four models compared

Experiment 2 was devised to test whether our model of detection thresholds generalizes to XOI in suprathreshold

conditions by measuring contrast discrimination. Using this paradigm, the effects of a superimposed cross-oriented mask have been examined at low spatial frequencies, where they are known to be suppressive (Foley, 1994; Holmes & Meese, 2004; Ross & Speed, 1991). And the effects of cross-oriented masks in the surround (or flanks) have been examined at high spatial frequencies, where they are thought to involve facilitation (Yu et al., 2002, 2003), or both facilitation and suppres-

sion (Chen & Tyler, 2002). But the results from Experiment 1 revealed novel insights into XOI for superimposed masks at high spatial frequencies. This motivated enquiry into the unchartered territory of pedestal plus superimposed masking at high spatial frequency. But what type of results might we expect? Figure 5 shows typical 'dipper functions' with and without a cross-oriented mask for four different model arrangements as follows (the parameter values are shown in Table 2).
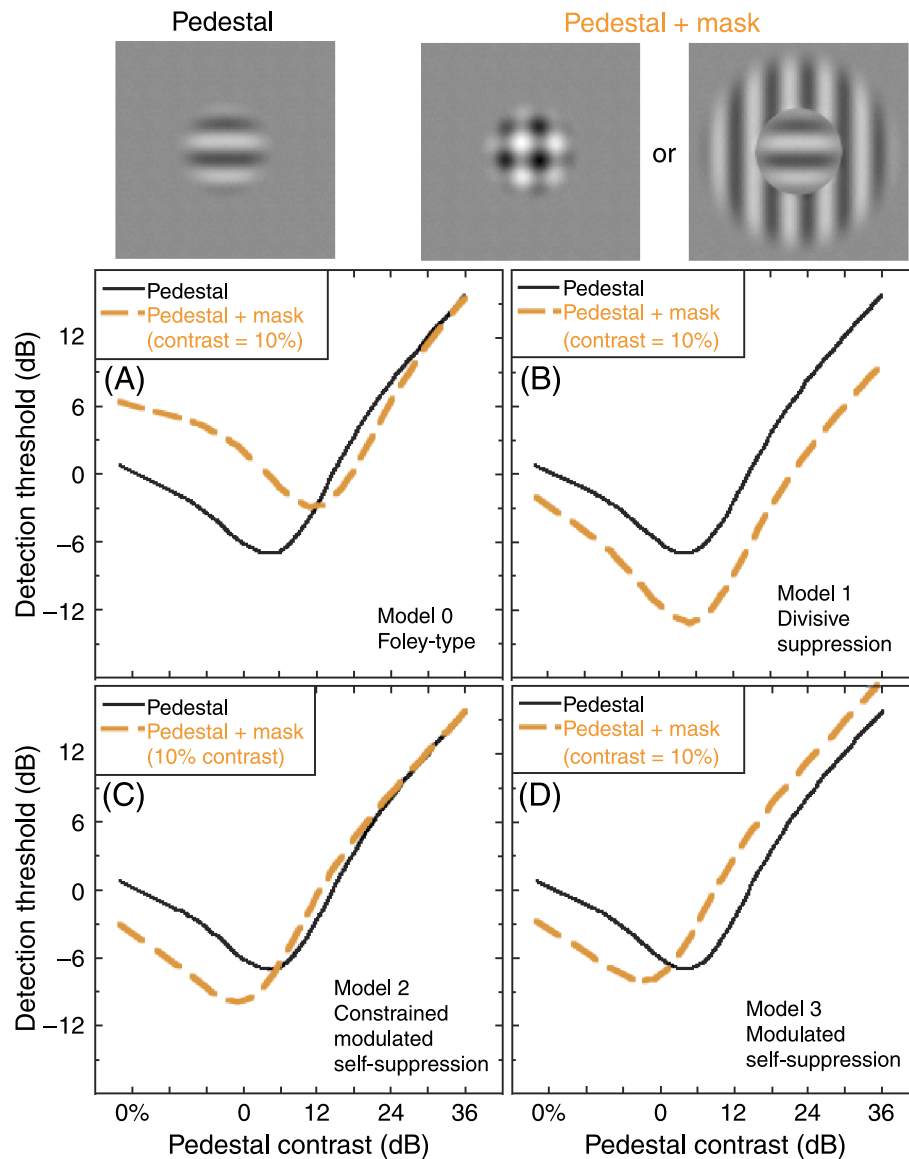

Figure 5. Canonical behaviors for four different models of pedestal masking (solid curve) in the presence of a fixed contrast cross-oriented mask (dashed curve). Whether the mask is superimposed or a doughnut is not explicit. The models are: (A) Model 0. Foley's (1994) low spatial frequency model (Equation 4). (B) Model 1. The divisive suppression model used in Experiment 1 (Equation 5). This has a similar form to the model considered by Yu et al. (2003). (C) Model 2. The constrained modulated self-suppression model, in which divisive suppression from the cross-oriented mask is replaced by modulation of the pedestal term on the denominator (Equation 6). (D) Model 3. The modulated self-suppression model is a generalization of Model 2, where in this instance the modulatory weight is heavier on the denominator than on the numerator (Equation 7). This last model is similar to one considered by Chen and Tyler (2002). Note that Model 0 is the only one that does not include modulatory facilitation from the cross-oriented mask.

	p	q	w	α	b	z	k
Model 0 (Foley, 1994, type)	2.4	2.0	0.2	n/a	n/a	5	0.2
Model 1 (divisive suppression: Yu, Klein, & Levi, 2001, type)	2.4	2.0	0	0.1	n/a	5	0.2
Model 2 (constrained modulated self-suppression)	2.4	2.0	n/a	0.2	n/a	5	0.2
Model 3 (modulated self-suppression: Chen & Tyler, 2002, type)	2.4	2.0	n/a	0.2	0.3	5	0.2

Table 2. Parameter values used to illustrate the canonical behavior (Figure 5) of the four models in Equations 4, 5, 6 and 7.

Foley type (Model 0)

Figure 5A is for a model introduced by Foley (1994), which has the form:

$$\text{resp} = \frac{c_{\text{ped}}^p}{z + c_{\text{ped}}^q + w c_{\text{xom}}^q}, \tag{4}$$

where c_{ped} refers to the contrast of the pedestal plus test increment (if it is present), and c_{xom} refers to the contrast of a cross-oriented mask. This version of Foley's model has a single divisive term for XOS, $w c_{\text{xom}}^q$ (w is a weight parameter), which adds to a self-suppression term c_{ped}^q and a saturation constant z on the denominator (Carandini & Heeger, 1994; Foley, 1994; Heeger, 1992; Tolhurst & Heeger, 1997). There is no provision for XOF. The model predicts that a superimposed mask shifts the dip region of the masking function upward, but that the 'dipper handles' converge at higher pedestal contrasts (Figure 5A). Thus, the cross-oriented mask produces masking at detection threshold, but facilitation by the pedestal survives this transformation. This model has been very successful at low spatial frequencies where cross-oriented masking is strong (Foley, 1994; Holmes & Meese, 2004). However, it is ruled out here by the results from Experiment 1, which show that when testing at 7 c/deg, superimposed cross-oriented masks produce facilitation, not masking.

Divisive suppression (Model 1)

Figure 5B shows the prediction for Model 1 (see earlier), with parameter values set to produce XOF at detection threshold.[2] This model can be re-expressed in the terms used here as follows:

$$\text{resp} = \frac{c_{\text{ped}}^p (1 + \alpha c_{\text{xom}})}{z + c_{\text{ped}}^q + w c_{\text{xom}}^q} \tag{5}$$

This extends the Foley-type model by including a modulatory term for XOF on the numerator. It predicts that the entire dipper function is translated downward by the mask, such that sensitivity is improved across the full range of pedestal contrasts (Figure 5B). This is the behavior found by Yu et al. (2002, 2003) for a cross-oriented mask in the surround at a spatial frequency of 8 c/deg. With $w = 0$, this model has a similar form to the one used by Yu et al. (2002), although they did not express the functional relation between mask contrast and the weight of modulation.

Constrained modulated self-suppression (Model 2)

Figure 5C shows the prediction for a conceptual modification to Model 1 as follows:

$$\text{resp} = \frac{c_{\text{ped}}^p (1 + \alpha c_{\text{xom}})}{z + c_{\text{ped}}^q (1 + \alpha c_{\text{xom}})}. \tag{6}$$

Note that in this equation, the modulatory term $(1 + \alpha c_{\text{xom}})$ from the numerator in Model 1 is now also applied to the pedestal (plus test) contrast on the denominator, replacing the previous divisive term αc_{xom}^q. This means that XOS is due to modulation of self-suppression and predicts facilitation at low pedestal contrasts followed by convergence of the 'dipper handles' at higher contrasts (Figure 5C). This pattern is the reverse of that produced by the Foley-type model (Figure 5A).

Modulated self-suppression (Model 3)

Finally, Figure 5D shows the prediction for a generalization of Model 2, as follows:

$$\text{resp} = \frac{c_{\text{ped}}^p (1 + \alpha c_{\text{xom}})}{z + c_{\text{ped}}^q (1 + b c_{\text{xom}})}. \tag{7}$$

In this model, the modulatory terms are permitted different weights on the numerator (α) and the denominator (b). With $b > \alpha$, This model predicts that facilitation occurs at low pedestal contrasts but gives way to further masking as pedestal contrast increases (Figure 5D). This is the behavior found by Chen and Tyler (2002) for pedestal masking in the presence of cross-oriented flanking masks at a spatial frequency of 4 c/deg. This model has a similar form to that used by Chen and Tyler (2002), although they did not express the functional relation between mask contrast and the weight of modulation.

As Models 1, 2, and 3 all produce facilitation at low pedestal contrasts (Figures 5B, 5C, and 5D), they are all viable candidates for Experiment 2 here.

The effect of cross-oriented masks on pedestal masking at 7c/deg

The results for the superimposed mask (Figures 1A and 1D) are shown for three observers in Figures 6A, C,
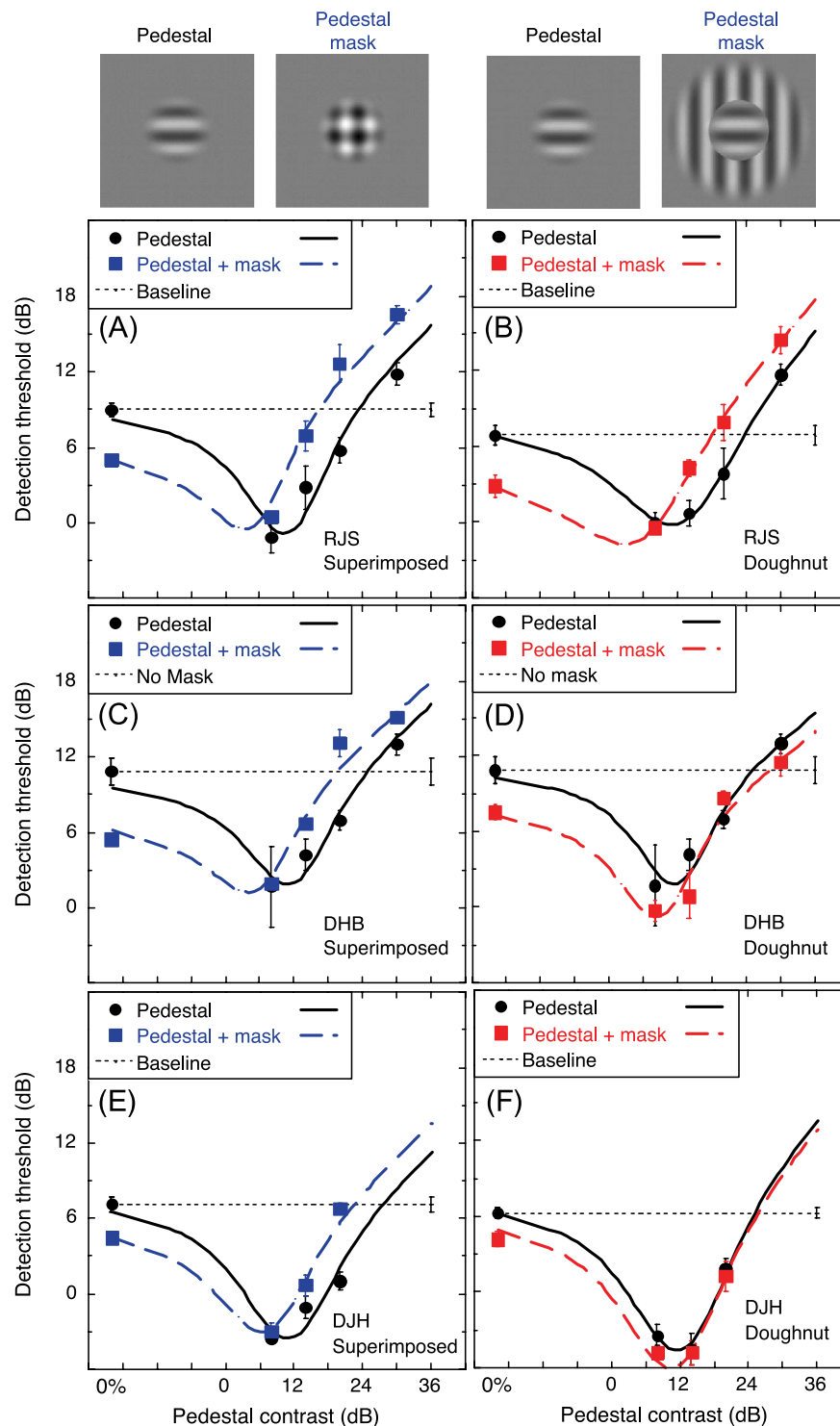
Figure 6. Pedestal masking (dipper) functions with (open symbols) and without (solid symbols) a fixed contrast cross-oriented mask of 10%. The fixed mask was either a small, superimposed patch (left) or a medium doughnut (right). Data are for RJS (top), DHB (middle), and DJH (bottom). Curves are fits of the modulated self-suppression model (Model 3) (see Table 3 for details). Each data point is estimated from ~400 trials. For DHB, the solid circular symbols plot the same data in the two panels. Error bars show ±1 *SE*.

and E. In all cases, they have the form predicted by the modulated self-suppression model (Model 3), for which the fit is shown by the solid curves (for details, see Table 3). DJH (Figure 6E) did not perform this experiment at the highest pedestal contrast, and so arguably the dipper

handles might have converged in that region (cf. Model 2; Figure 5C), although for the other two observers this clearly does not happen (Figures 6A and C). Furthermore, for neither observer is there any suggestion that the facilitation extends across the entire dipper region as in

Observer	Fixed mask	RMS error (dB)	p	q	α	b	z	k	α/b
RJS	Superimposed	1.043	3.11	2.59	0.323	0.494	32.87	0.436	0.65
DHB	Superimposed	1.027	2.98	2.42	0.321	0.417	20.99	0.591	0.77
DJH	Superimposed	0.841	2.82	2.28	0.119	0.184	22.50	0.304	0.65
RJS	Doughnut	0.238	2.22	1.76	0.233	0.330	15.66	0.292	0.71
DHB	Doughnut	1.017	3.35	2.75	0.22	0.17	51.58	0.690	1.29
DJH	Doughnut	0.449	2.66	2.28	0.048	0.037	30.06	0.196	1.32

Table 3. Parameter values and other details of the fits of the modulated self-suppression model to the results from Experiment 2. The ratio α/b was used in testing the hybrid model (Model 4).

Figure 5B. Thus, Models 1 and 2 cannot describe contrast discrimination in the presence of a superimposed mask at high spatial frequencies without modification.

This result was surprising because Yu et al. (2002, 2003) found results like those in Figure 5B (Model 1) when the mask was limited to the surround. To see whether different results are found for superimposed and surround masks, we performed the experiment again, but in the presence of a doughnut mask (Figures 1A and 1B). For RJS, the pattern of results (Figure 6B) is very similar to the superimposed case and not at all like those of Yu et al. (2002, 2003). For DHB and DJH the effect of the surround mask was weak in this experiment, meaning that their data do not very well decide between the three candidate models. Nevertheless, good fits to the data were achieved for both observers using Model 3 (see Table 3 for details), the same as for the superimposed case. Thus, it is now clear that the cross-orientation modulation observed by Chen and Tyler (2002) from flanking patches is not restricted to influences from outside the receptive field of the detecting mechanism.

Model 4: A hybrid of Model 1 and Model 3

The reader who is not concerned with the functional details of the modelling could skip over this subsection to Section 5 without loss of continuity.

Model 1 was very successful in describing the results at detection threshold in Experiment 1, but the results from Experiment 2 reject it in preference for Model 3. However, that model is not suitable (and was not designed) for the results from either Experiment 1 or other experiments where cross-orientation masking dominates at low spatial frequencies (e.g., Foley, 1994). The main problem with Model 3 is that its suppressive influence comes from cross-orientation modulation of self-suppression; this is the c_{ped} term (the pedestal + test contrast) on the denominator of Equation 7. For stimuli with no pedestal (e.g., those in Experiment 1), this term is small, the model equation is dominated by the saturation constant z, and there is little or no masking. This can be overcome by using very large values of b, but this leads to other problems. It means the model does not produce convergence of the dipper handles in pedestal plus fixed mask experiments (see Figure 5A),

which is known to happen at low spatial frequencies (Foley, 1994; Holmes & Meese, 2004; Ross & Speed, 1991). Furthermore, the arrangement of modulation on both numerator and denominator means that the model does not describe the decline of facilitation after its onset (see Figure 3).

A possible solution to this general dilemma is a model that includes all the features of the two successful models from Experiments 1 and 2. We refer to this as the hybrid model (Model 4), which is expressed as follows:

$$\text{resp} = \frac{c_{ped}^{p}(1 + \alpha_{center}c_{xcenter} + \alpha_{surround}c_{xsurround})}{z + c_{ped}^{q}(1 + b_{center}c_{xcenter} + b_{surround}c_{xsurround}) + w_{center}c_{xcenter}^{q} + w_{surround}c_{xsurround}^{q}}.$$

(8)

Note that this model includes two routes to suppression on the denominator. One is controlled by w and represents divisive suppression from the mask (as in Model 1). The other is controlled by b and represents modulation of self-suppression by the mask (as in Model 3). The route to facilitation is the same as for Models 1–3. The hybrid model was fitted to the results from both experiments (not shown) to determine whether the various types of interaction interfere with each other. In doing this, the number of free parameters was constrained to be the same as for Model 1 in Experiment 1 and Model 3 in Experiment 2.

For Experiment 1, we constrained $b = \alpha/0.65$ for the center and $b = \alpha/1.32$ for the surround, consistent with the extremes of these parameters in Experiment 2 (last column of Table 1). This is probably over-restrictive for the low spatial frequency conditions from Experiment 1, where we have no estimates of α and b. Nevertheless, we found only marginal changes in the quality of the fit for the hybrid model (not shown). For Experiment 2, when $w > 0$, this adds a constant to the denominator of the model equation (equivalent to increasing the magnitude of z). So long as w was not so large that it overpowered the facilitation produced by α at threshold, we found that it had negligible impact on the fitting (not shown).

The tests above are encouraging for Model 4, which is the only one of the five models (Models 0–4) that can fit all of the results from both of our experiments. However, as a general equation it should be treated with some caution. This

is because some of its features derive from the hybridization of the two earlier models, but for which we have no direct evidence. For example, we have not performed experiments that bear on the summation of the modulatory b terms from the center and the surround. Furthermore, Experiment 1 suggests that the functional relation between mask contrast and facilitatory modulation is a reasonable one at detection threshold, but we do not know whether this relation extends well above threshold. Similarly, we have not tested the functional relation between mask contrast and the modulation of self-suppression.

Discussion

Summary of main findings

In Experiment 1, we investigated the effects of mask contrast on detection thresholds for several different mask configurations. We found that results differed markedly across spatial frequency and mask region. We developed a functional model of the results (Model 1, Equation 3) involving facilitatory modulation and divisive suppression from both center and surround. This allowed us to estimate the strengths of XOI from center and surround and across spatial frequency, as shown in Figure 4. Experiment 2 extended the investigation above threshold by placing the test increment on a pedestal. This showed that cross-oriented masks also modulate the strength of self-suppression (i.e., suppression from the pedestal contrast) at high spatial frequencies (Model 3). The processes revealed by the two experiments were combined in a single hybrid model (Model 4), which provided good fits to all of our data.

In sum, a model in which XOS and XOF arise from masks in both center and surround accounts for a wide range of results across conditions and observers. Thus, although XOF was once thought to be a process specific to the surround (Cavanaugh et al., 2002b; Chen & Tyler, 2002; Jones et al., 2002; Yu & Levi, 2000), it is now clear that it extends across the central region as well (cf. Webb et al., 2005).

Comparisons with other psychophysical studies

A result that can be seen from direct observation of the data (Experiment 1, Figures 2 and 3) as well as the modelling (Figure 4) is the profound loss of XOS with increasing spatial frequency; our parallel study (Meese & Holmes, 2007) explored this in more detail and found similar results. Meese and Holmes (2007) measured detection thresholds for Gabor tests and superimposed orthogonal Gabor masks (similar to the SS configuration here) for a wide range of spatiotemporal frequencies for the same observers. They achieved very good fits to the data using Equations 1 and 3 (here), with the facilitatory weight (α) fixed across spa-

tiotemporal frequency. They found that the suppressive weight (w) decreased in proportion to the ratio of spatial frequency to temporal frequency (on double log axes).

This large effect of spatial frequency on the behavior of XOI is partly responsible for some previous discrepancies in the literature (e.g., Meese, 2004; Yu et al., 2002). However, the nonlinearities in the model also play an important role. Although center and surround terms are summed on both the numerator and denominator of Equation 3, this does not translate into summation of their effects. For example, there are distinct regions of facilitation produced by the surround in the doughnut masks for observers DHB and BX at 1 c/deg (conditions DM and DL in Figure 2). However, a comparison of the different sized superimposed conditions for the same observers reveals that when a superimposed small mask (SS) is extended to the surround (SM and SL), the surround has little or no affect (see also Meese, 2004). Or put another way, facilitation from the surround is no longer seen in the data or model when the mask is extended over the center, although the facilitatory process remains intact in the model.

In our second experiment, we found further evidence for processes of XOI that are similar for masks placed in the center and the surround. However, these results conflict with those of Yu et al. (2003) who performed experiments similar to our doughnut configuration in Experiment 2. The pattern of their results was like that in Figure 5B (see also Yu et al., 2002), whereas ours was more like that in Figure 5D (RJS) and arguably Figure 5C (DHB and DJH). Both studies were performed at similar spatial frequencies (7 and 8 c/deg) and with similar stimulus durations (200 and 300 ms). There were two main differences between the studies. The first is the fixation regimen. Yu et al. used a central fixation point that was extinguished before each trial, whereas we used a quad of fixation points that surrounded the outer region of the medium sized mask and were displayed continuously. If the fixation marks were in some way involved in modulating XOI in one of the studies then this could be responsible for the different results. The second difference concerns the details of stimulus construction. Yu et al. used a pedestal that was slightly larger than the test patch whereas our pedestal was the same as the test patch. Thus in Yu et al.'s experiment there were three sources of masking to consider: (i) the variable pedestal contrast, and incremental test contrast when present; (ii) the surrounding pedestal contrast for which there was never an increment; and (iii) the outer surrounding cross-oriented mask with fixed contrast. Yu et al.'s analysis considered only sources (i) and (iii). It remains unclear whether source (ii) is responsible for the discrepancy in the results. Observer differences between the studies, reflecting different parameter weights in Model 4, might also be important. We do note, however, that Chen and Tyler (2002) found a very similar pattern of results to us (Figure 5D) using cross-oriented fixed contrast masks that were restricted to flanking patches in the surround.

Facilitation by reduction of uncertainty?

We have described our results with a model involving facilitatory interactions between mask and test mechanisms. However, another process that can produce facilitation is reduction of uncertainty (Pelli, 1985). The idea is that the mask provides the observer with information about stimulus details including spatial frequency, orientation and spatial location (Petrov et al., 2006; Williams & Hess, 1998). This reduces the number of mechanisms that the observer needs to monitor and facilitates detection because of the concomitant reduction in overall noise (Pelli, 1985). However, there is little room for reduction of uncertainty in our experiments. The fixation points (central at 1 c/deg and a quad at 7 c/deg) were visible throughout and provided a strong cue to spatial location. One set of results that presents a particularly strong challenge for the uncertainty hypothesis is that for observer BX (Figure 2D) where the doughnut mask provides facilitation over a wide range of mask contrasts. The target was a 2° patch of 1 c/deg grating for which there could have been little or no spatial uncertainty owing to its size and the central fixation point. The mask could not reduce uncertainty about spatial frequency and orientation as it differed the target substantially in both of these dimensions. Another strong challenge is presented by the results of observer DJH (Figure 3C). Here the target was a small (0.29°) patch of 7 c/deg grating. Lets suppose that in spite of the quad fixation points there was some spatial uncertainty for this patch. This could be reduced by a small, superimposed mask of similar size to the target, or a doughnut with a hole of similar size to the target. Indeed, these conditions both produced facilitation. But a very similar level of facilitation occurred for a superimposed mask with a diameter of 8° (blue squares). As the diameter of the mask is 28 times that of the test patch, it is implausible that it reduced spatial uncertainty.

Finally, reduction of uncertainty can produce facilitatory effects only at detection threshold. Nevertheless, there is evidence that masks can enhance perceived contrast, which requires a sensory process (although the effects are quite small). Xing and Heeger (2001) and Yu et al. (2001) found this for doughnut masks and Meese and Hess (2004) found it for a superimposed mask from a different spatial frequency and orientation band. There is also single-cell evidence for suprathreshold facilitatory interactions from cross-oriented surrounds in striate cortex (Cavanaugh et al., 2002b).

In sum, we cannot rule out the possibility that reduction of uncertainty contributes to the facilitation seen here, but we doubt that it is the sole cause. Similarly, Petrov et al. (2006) recognized that reduction of uncertainty was probably not the sole cause of the flanker facilitation in their study.

Two forms of XOS

Our experiments indicate two distinct forms of XOS. The first (Experiment 1) involves direct divisive suppression of the detecting mechanism by the cross-oriented mask. For a fixed-contrast mask this is equivalent to increasing the size of the saturation constant (z). This has the effect of depressing the contrast response at lower test contrasts but leaving it intact at higher contrasts. We refer to this as divisive suppression. The second (Experiment 2) involves modulation of self-suppression by the cross-oriented mask. For a fixed-contrast mask, this has the effect of leaving the contrast response intact at lower contrasts, but depressing it at higher contrasts. We refer to this as modulated self-suppression. The combined effect of divisive suppression and modulated self-suppression is to depress the contrast response across the entire operating characteristic of the detecting mechanism. Of course, this could be achieved more directly by modulating the sum of the saturation constant and self-suppression by a single function of mask contrast. However, the results here and elsewhere indicate that the two processes must act independently. This is because divisive suppression dominates at low spatial frequencies (Foley, 1994; Holmes & Meese, 2004), whereas modulated self-suppression dominates at high spatial frequencies. This need for independence can be seen in the results from Experiment 2. If cross-oriented mask contrast modulated the entire denominator of the model equation with weight b, then the mask would shift the entire dipper functions in Experiment 2 (Figure 6) either upward or downward, depending on the relative values of b and the facilitatory weight α. This is not what we found.

There is a parallel to be drawn between the two types of XOS seen here, and two forms of XOS found by Sengpiel, Baddeley, Freeman, Harrad, and Blakemore (1998) at the single-cell level. Sengpiel et al. defined "response gain control" as the depression of a cell's contrast response, which is similar to the modulated self-suppression here. A second type of suppression found by Sengpiel et al. (1998) was "contrast gain control," which was equivalent to changing the magnitude of the semi-saturation constant in their gain-control equation, rather like our divisive suppression here. Sengpiel et al. found "contrast gain control" for monoptic cross-oriented masking (mask and test presented to the same eye) and "response gain control" for dichoptic cross-oriented masking (mask and test presented to different eyes). Thus, it is possible that the two forms of suppression seen here-represent the monoptic and dichoptic influences of XOS that one might suppose would be tapped by our binocular stimuli.

The purpose of XOI?

Cross-orientation interactions (XOI) are a fundamental property of mammalian early vision. In Section 1, we summarized some of the suggestions that have been made for why they might occur. But do our results have any impact on these ideas?

In the case of XOS, we found two effects. The divisive suppression from Experiment 1 showed a profound de-

crease with spatial frequency, consistent with the results from our parallel study (Meese & Holmes, 2007). The suggestion in that study was that higher spatial frequencies are probably processed preferentially by the parvocellular subsystem (Lennie & Movshon, 2005; Merigan, Katz, & Maunsell, 1991). The cells in that stream are more linear than those in the magnocellular stream (Derrington & Lennie, 1984) and in less need of contrast normalization through XOS to preserve population codes in the face of saturation (Albrecht & Geisler, 1991; Heeger, 1992). The results here are consistent with that view.

The modulated self-suppression from Experiment 2 was evident only when the pedestal contrast was above detection threshold. It remains unclear whether this augments or interferes with the process of contrast normalization and whether it operates at low spatial frequencies.

The purpose of XOF is also unclear. One suggestion is that XOF from the surround might help perform object segmentation at texture boundaries by highlighting orientation discontinuities (Sillito et al., 1995), although suppression from a parallel surround is another way of achieving this (Grigorescu et al., 2004). Our results do not rule out the possibility that there is a class of cell in primary visual cortex that is dedicated to detecting orientation discontinuities (Sillito et al., 1995), but it seems unlikely that this is the process revealed here. This is because the facilitation is not restricted to comparisons across center and surround, which defies the requirements of a process intended for spatial comparisons.

Spatial architecture of XOI

A natural interpretation of our functional models is that sources of XOI arise from cross-oriented mechanisms with receptive fields centered over the center and surround regions of the test mechanism. However, there are other possibilities. It could be that all of the effects arise from a centrally placed cross-oriented mechanism that has a sufficiently large receptive field to respond to cross-oriented masks placed in either the center or the surround. A less extreme proposal is that XOI are mediated by multiple mechanisms with fairly small receptive fields (≤ 2 cycles). If the centers of these receptive fields were all within the receptive field of a similarly sized detecting mechanism then their skirts would extend into the surround, resulting in only weak effects from that region. In fact, this is what we found at low spatial frequencies. However, at high spatial frequencies the strengths of the interactions were similar in both regions, suggesting that XOI involves mechanisms whose centers are outside the receptive field of the detecting mechanism.

A general scheme consistent with our data is depicted in Figure 7, which shows the arrangement of cross-orientation interactions for a central detecting mechanism. The strength of XOF (thickness of green/pale arrows) does not change with spatial frequency, whereas the strength of XOS (thickness of red/dark arrows) is weaker at the higher spatial frequencies. XOI arise from the origins of red and green arrows and are similar at low (Figure 7A) and high (Figure 7B) spatial frequencies, although there is some uncertainty about
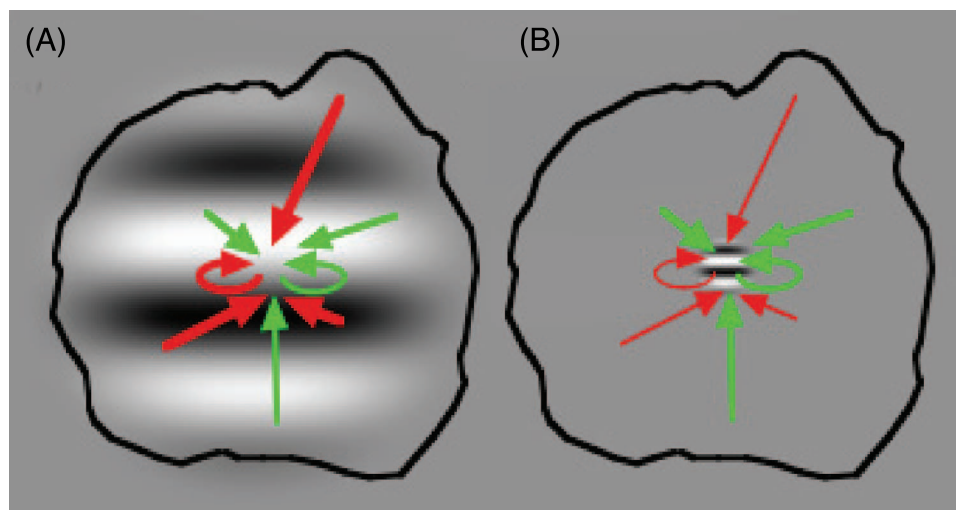

Figure 7. Spatial arrangements and strengths of cross-orientation interactions (XOI) for a centrally placed detecting mechanism. The green (pale) and red (dark) arrows denote spatial interactions that are facilitatory and suppressive respectively and have the same arrangement at both spatial frequencies (A and B). The thickness of each arrow indicates the weight of the interaction. The grating patches indicate the relative sizes of the 1 c/deg (A) and 7 c/deg (B) stimuli used in our experiments and are probably a little larger than the classical receptive fields of the underlying detecting mechanisms. The wiggly black closed curves indicate that there is some uncertainty about the precise size of the spatial region from which the interactions arise. Nevertheless, at high spatial frequencies (B) the interactions operate over a greater number of stimulus cycles than at low spatial frequencies (A).

the boundaries (the wiggly black contours). Nevertheless, if XOI arise from similar spatial extents at all spatial frequencies then for doughnut masks they will be seen principally at higher spatial frequencies, just as we found.

Conclusions

The most parsimonious account of our results supposes ubiquitous processes of excitatory and suppressive interactions between cross-oriented mechanisms over a spatial extent that exceeds receptive field size at higher spatial frequencies. Different weights for these two processes across observer, spatial frequency, and spatial origin account for the full variety of psychophysical results seen here and elsewhere.

Acknowledgments

Commercial relationships: none.
Corresponding author: Tim S. Meese.
E-mail: t.s.meese@aston.ac.uk.
Address: Neurosciences Research Institute, Aston University, Aston Triangle, Birmingham B4 7ET, UK.

Footnote

[1]Elsewhere (Meese & Holmes, 2007) we have found it convenient to use the terms cross-orientation masking (XOM) and cross-orientation facilitation (XOF) to refer to psychophysical phenomena and cross-orientation suppression (XOS) and cross-orientation enhancement (XOE) to refer to the underlying processes. We do not use this terminology to make that distinction here, but use the terms XOS and XOF to refer to two different classes of modulatory interaction (suppressive and facilitatory). More generally, we use the term cross-orientation interactions (XOI) to refer to both or either of these.

[2]Here we have set $w = 0$ (Table 2), but this is not crucial for our point. So long as w is sufficiently small for XOF to remain intact at detection threshold, performance is facilitated across the entire dipper function.

References

Abbey, C. K., & Eckstein, M. P. (2006). Classification images for detection, contrast discrimination, and iden- tification tasks with a common ideal observer. *Journal of Vision, 6*(4):4, 335–355, http://journalofvision.org/6/4/4/, doi:10.1167/6.4.4. [PubMed] [Article]

Albrecht, D. G., & Geisler, W. S. (1991). Motion selectivity and the contrast–response function of simple cells in the visual cortex. *Visual Neuroscience, 7*, 531–546. [PubMed]

Bair, W., Cavanaugh, J. R., & Movshon, J. A. (2003). Time course and time–distance relationships for surround suppression in macaque V1 neurons. *The Journal of Neuroscience, 23*, 7690–7701. [PubMed] [Article]

Baker, D. H., & Meese, T. S. (2006). Cross-orientation suppression occurs before binocular summation: Evidence from masking and adaptation [Abstract]. *Journal of Vision, 6*(6):821, 821a, http://journalofvision.org/6/6/821/, doi:10.1167/6.6.821.

Baker, D. H., Meese, T. S., & Georgeson, M. A. (in press). Binocular interaction: Contrast matching and contrast discrimination are predicted by the same model. *Spatial Vision.*

Baker, D. H., Meese, T. S., & Summers, R. J. (in press). Psychophysical evidence for two routes to suppression before binocular summation of signals in human vision. *Neuroscience.*

Bonds, A. B. (1989). Role of inhibition in the specification of orientation selectivity of cells in the cat striate cortex. *Visual Neuroscience, 2*, 41–55. [PubMed]

Bonin, V., Mante, V., & Carandini, M. (2005). The suppressive field of neurons in lateral geniculate nucleus. *The Journal of Neuroscience, 25*, 10844–10856. [PubMed] [Article]

Born, R. T., & Tootell, R. B. (1991). Single-unit and 2-deoxyglucose studies of side inhibition in macaque striate cortex. *Proceedings of the National Academy of Sciences of the United States of America, 88*, 7071–7075. [PubMed] [Article]

Bruce, V., Green, P. R., & Georgeson, M. A. (2003). *Visual perception: Physiology, psychology and ecology* (4th Ed.), Hove: Psychology Press.

Burr, D. C., & Morrone, M. C. (1987). Inhibitory interactions in the human vision system revealed in pattern-evoked potentials. *The Journal of Physiology, 389*, 1–21. [PubMed] [Article]

Cannon, M. W., & Fullenkamp, S. C. (1991). Spatial interactions in apparent contrast: Inhibitory effects among grating patterns of different spatial frequencies, spatial positions and orientations. *Vision Research, 31*, 1985–1998. [PubMed]

Cannon, M. W., & Fullenkamp, S. C. (1993). Spatial interactions in apparent contrast: Individual differences in enhancement and suppression effects. *Vision Research, 33*, 1685–1695. [PubMed]

Carandini, M., Demb, J. B., Mante, V., Tolhurst, D. J., Dan, Y., Olshausen, B. A., et al. (2005). Do we know what the early visual system does? *The Journal of Neuroscience, 25,* 10577–10597. [PubMed] [Article]

Carandini, M., & Heeger, D. J. (1994). Summation and division by neurons in primate visual cortex. *Science, 264,* 1333–1336. [PubMed]

Cavanaugh, J. R., Bair, W., & Movshon, J. A. (2002a). Nature and interaction of signals from receptive field center and surround in macaque V1 neurons. *Journal of Neurophysiology, 88,* 2530–2546. [PubMed] [Article]

Cavanaugh, J. R., Bair, W., & Movshon, J. A. (2002b). Selectivity and spatial distribution of signals from the receptive field surround in macaque V1 neurons. *Journal of Neurophysiology, 88,* 2547–2556. [PubMed] [Article]

Chen, C. C., & Tyler, C. W. (2001). Lateral sensitivity modulation explains the flanker effect in contrast discrimination. *Proceedings of the Royal Society B: Biological Sciences, 268,* 509–516. [PubMed] [Article]

Chen, C. C., & Tyler, C. W. (2002). Lateral modulation of contrast discrimination: Flanker orientation effects. *Journal of Vision, 2*(6):8, 520–530, http://journalofvision.org/2/6/8/, doi:10.1167/2.6.8. [PubMed] [Article]

Cornsweet, T. N. (1962). The staircase-method in psychophysics. *The American Journal of Psychology, 75,* 485–491. [PubMed]

DeAngelis, G. C., Robson, J. G., Ohzawa, I., & Freeman, R. D. (1992). Organization of suppression in receptive fields of neurons in cat visual cortex. *Journal of Neurophysiology, 68,* 144–163. [PubMed]

Derrington, A. M., & Lennie, P. (1984). Spatial and temporal contrast sensitivities of neurones in lateral geniculate nucleus of macaque. *The Journal of Physiology, 357,* 219–240. [PubMed] [Article]

DeValois, R. L., & DeValois, K. K. (1988). *Spatial vision.* Oxford: Oxford University Press.

Dorais, A., & Sagi, D. (1997). Contrast masking effects change with practice. *Vision Research, 37,* 1725–1733. [PubMed]

Ejima, Y., & Takahashi, S. (1985). Apparent contrast of a sinusoidal grating in the simultaneous presence of peripheral gratings. *Vision Research, 25,* 1223–1232. [PubMed]

Felsen, G., Touryan, J., & Dan, Y. (2005). Contextual modulation of orientation tuning contributes to efficient processing of natural stimuli. *Network, 16,* 139–149. [PubMed]

Field, D. J., Hayes, A., & Hess, R. F. (1993). Contour integration by the human visual system: Evidence for a local "association field." *Vision Research, 33,* 173–193. [PubMed]

Foley, J. M. (1994). Human luminance pattern-vision mechanisms: Masking experiments require a new model. *Journal of the Optical Society of America A, Optics, Image Science, and Vision, 11,* 1710–1719. [PubMed]

Foley, J. M., & Chen, C. C. (1997). Analysis of the effect of pattern adaptation on pattern pedestal effects: A two-process model. *Vision Research, 37,* 2779–2788. [PubMed]

Freeman, E., Driver, J., Sagi, D., & Zhaoping, L. (2003). Top-down modulation of lateral interactions in early vision: Does attention affect integration of the whole or just perception of the parts? *Current Biology, 13,* 985–989. [PubMed] [Article]

Freeman, T., Durand, S., Kiper, D., & Carandini, M. (2002). Suppression without inhibition in visual cortex. *Neuron, 35,* 759–771. [PubMed] [Article]

García-Pérez, M. A., & Peli, E. (2001). Luminance artefacts of cathode-ray tube displays for vision research. *Spatial Vision, 14,* 201–215. [PubMed]

Grigorescu, C., Petkov, N., & Westenberg, M. A. (2004). Contour and boundary detection improved by surround suppression of texture edges. *Image and Vision Computing, 22,* 609–622.

Guo, K., Robertson, R. G., Mahmoodi, S., & Young, M. P. (2005). Centre–surround interactions in response to natural scene stimulation in the primary visual cortex. *European Journal of Neuroscience, 21,* 536–548. [PubMed]

Heeger, D. J. (1992). Normalization of cell responses in cat striate cortex. *Visual Neuroscience, 9,* 181–197. [PubMed]

Hegdé, J., & Felleman, D. J. (2003). How selective are V1 cells for pop-out stimuli? *The Journal of Neuroscience, 23,* 9968–9980. [PubMed] [Article]

Hess, R. F., Dakin, S. C., & Field, D. J. (1998). The role of "contrast enhancement" in the detection and appearance of visual contours. *Vision Research, 38,* 783–787. [PubMed]

Holmes, D. J., & Meese, T. S. (2004). Grating and plaid masks indicate linear summation in a contrast gain pool. *Journal of Vision, 4*(12):7, 1080–1089, http://journalofvision.org/4/12/7/, doi:10.1167/4.12.7. [PubMed] [Article]

Huang, P. C., Hess, R. F., & Dakin, S. C. (2006). Flank facilitation and contrast integration: Different sites. *Vision Research, 46,* 3699–3706. [PubMed]

Hubel, D. H., & Wiesel, T. N. (1959). Receptive fields of single neurones in the cat's striate cortex. *The Journal of Physiology, 148,* 574–591. [PubMed] [Article]

Hubel, D. H., & Wiesel, T. N. (1962). Receptive fields, binocular integration and functional architecture in the cat's visual cortex. *The Journal of Physiology, 160,* 106–154. [PubMed] [Article]

Ishikawa, A., Shimegi, S., & Sato, H. (2006). Metacontrast masking suggests interaction between visual pathways

with different spatial and temporal properties. *Vision Research, 46,* 2130–2138. [PubMed]

Jones, H. E., Grieve, K. L., Wang, W., & Sillito, A. M. (2001). Surround suppression in primate V1. *Journal of Neurophysiology, 86,* 2011–2028. [PubMed] [Article]

Jones, H. E., Wang, W., & Sillito, A. M. (2002). Spatial organization and magnitude of orientation contrast interactions in primate V1. *Journal of Neurophysiology, 88,* 2796–2808. [PubMed] [Article]

Jones, J. P., & Palmer, L. A. (1987). An evaluation of the two-dimensional Gabor filter model of simple receptive fields in cat striate cortex. *Journal of Neurophysiology, 58,* 1233–1258. [PubMed]

Kapadia, M. K., Ito, M., Gilbert, C. D., & Westheimer, G. (1995). Improvements in visual sensitivity by changes in local context: Parallel studies in human observers and in V1 of Alert Monkeys. *Neuron, 15,* 843–856. [PubMed] [Article]

Kurki, I., Hyvärinen, A., & Laurinen, P. (2006). Collinear context (and learning) change the profile of the perceptual filter. *Vision Research, 46,* 2009–2014. [PubMed]

Legge, G. E., & Foley, J. M. (1980). Contrast masking in human vision. *Journal of the Optical Society of America, 70,* 1458–1471. [PubMed]

Lennie, P., & Movshon, J. A. (2005). Coding of colour and form in the geniculostriate visual pathway (invited review). *Journal of the Optical Society of America A, Optics, Image Science, and Vision, 22,* 2013–2033. [PubMed]

Levitt, J. B., & Lund, J. S. (1997). Contrast dependence of contextual effects in primate visual cortex. *Nature, 387,* 73–76. [PubMed]

Li, B., Thompson, J. K., Duong, T., Peterson, M. R., & Freeman, R. D. (2006). Origins of cross-orientation suppression in the visual cortex. *Journal of Neurophysiology, 96,* 1755–1764. [PubMed]

Macknik, S. L., & Martinez-Conde, S. (2004). Dichoptic visual masking reveals that early binocular neurons exhibit weak interocular suppression: Implications for binocular vision and visual awareness. *Journal of Cognitive Neuroscience, 16,* 1049–1059. [PubMed]

Meese, T. S. (2004). Area summation and masking. *Journal of Vision, 4*(10):8, 930–943, http://journalofvision.org/4/10/8/, doi:10.1167/4.10.8. [PubMed] [Article]

Meese, T. S., & Hess, R. F. (2004). Low spatial frequencies are suppressively masked across spatial scale, orientation, field position, and eye of origin. *Journal of Vision, 4*(10):2, 843–859, http://journalofvision.org/4/10/2/, doi:10.1167/4.10.2. [PubMed] [Article]

Meese, T. S. Hess, R. F., & Williams, B. W. (2005). Size matters, but not for everyone: Individual differences for contrast discrimination. *Journal of Vision,* *5*(11):2, 928–947, http://journalofvision.org/5/11/2/, doi:10.1167/5.11.2. [PubMed] [Article]

Meese, T. S., & Holmes, D. J. (2002). Adaptation and gain pool summation: Alternative models and masking data. *Vision Research, 42,* 1113–1125. [PubMed]

Meese, T. S., & Holmes, D. J. (2006). Cross-orientation suppression is proportional to the square-root of speed for flickering Gabor stimuli [Abstract]. *Journal of Vision, 6*(6):200, 200a, http://journalofvision.org/6/6/200/, doi:10.1167/6.6.200.

Meese, T. S., & Holmes, D. J. (2007). Spatial and temporal dependencies of cross-orientation suppression in human vision. *Proceedings of the Royal Society B: Biological Sciences, 274,* 127–136. [PubMed]

Merigan, W. H., Katz, L. M., & Maunsell, J. H. (1991). The effects of parvocellular lateral geniculate lesions on the acuity and contrast sensitivity of macaque monkeys. *The Journal of Neuroscience, 11,* 994–1001. [PubMed] [Article]

Morrone, M. C., Burr, D. C., & Maffei, L. (1982). Functional implications of cross-orientation inhibition of cortical visual cells I. Neurophysiological evidence. *Proceedings of the Royal Society of London Series B, 216,* 335–354. [PubMed]

Morrone, M. C., Burr, D. C., & Speed, H. D. (1987). Cross-orientation inhibition in cat is GABA mediated. *Experimental Brain Research, 67,* 635–644. [PubMed]

Nelson, J. I., & Frost, B. J. (1985). Intracortical facilitation among co-oriented, co-axially aligned simple cells in cat striate cortex. *Experimental Brain Research, 61,* 54–61. [PubMed]

Ohtani, Y., Okamura, S., Yoshida, T., Toyama, K., & Ejima, Y. (2002). Surround suppression in the human visual cortex: An analysis using magnetoencephalography. *Vision Research, 42,* 1825–1835. [PubMed]

Olshausen, B. A., & Field, D. J. (2005). How close are we to understanding V1? *Neural Computation, 17,* 1665–1699. [PubMed]

Olzak, L. A., & Laurinen, P. I. (1999). Multiple gain control processes in contrast–contrast phenomena. *Vision Research, 39,* 3983–3987. [PubMed]

Olzak, L. A., & Laurinen, P. I. (2005). Contextual effects in fine spatial discriminations. *Journal of the Optical Society of America A, Optics, Image Science, and Vision, 22,* 2230–2238. [PubMed] [Article]

Ozeki, H., Sadakane, O., Akasaki, T., Naito, T., Shimegi, S., & Sato, H. (2004). Relationship between excitation and inhibition underlying size tuning and contextual modulation in the cat primary visual cortex. *The Journal of Neuroscience, 24,* 1428–1438. [PubMed] [Article]

Pelli, D. G. (1985). Uncertainty explains many aspects of visual contrast detection and discrimination. *Journal of the Optical Society of America A, Optics, Image Science, and Vision, 2,* 1508–1532. [PubMed]

Petrov, Y., Carandini, M., & McKee, S. (2005). Two distinct mechanisms of suppression in human vision. *The Journal of Neuroscience, 25,* 8704–8707. [PubMed] [Article]

Petrov, Y., & McKee, S. P. (2006). The effect of spatial configuration on surround suppression of contrast sensitivity. *Journal of Vision, 6*(3):4, 224–238, http://journalofvision.org/6/3/4/, doi:10.1167/6.3.4. [PubMed] [Article]

Petrov, Y., Verghese, P., & McKee, S. P. (2006). Collinear facilitation is largely uncertainty reduction. *Journal of Vision, 6*(2):8, 170–178, http://journalofvision.org/6/2/8/, doi:10.1167/6.2.8. [PubMed] [Article]

Polat, U. (1999). Functional architecture of long-range perceptual interactions. *Spatial Vision, 12,* 143–162. [PubMed]

Polat, U., & Sagi, D. (1993). Lateral interactions between spatial channels: Suppression and facilitation revealed by lateral masking experiments. *Vision Research, 33,* 993–999. [PubMed]

Priebe, N. J., & Ferster, D. (2006). Mechanisms underlying cross-orientation suppression in cat visual cortex. *Nature Neuroscience, 9,* 552–561. [PubMed]

Robson, J. G. (1980). Neural images: The physiological basis of spatial vision. In C. S. Harris (Ed.), *Visual coding and adaptability* (pp. 177–214). New Jersey: LEA.

Ross, J., & Speed, H. D. (1991). Contrast adaptation and contrast masking in human vision. *Proceedings of the Royal Society B: Biological Sciences, 246,* 61–69. [PubMed]

Sakai, K., & Nishimura, H. (2006). Surrounding suppression and facilitation in the determination of border ownership. *Journal of Cognitive Neuroscience, 18,* 562–579. [PubMed]

Schwartz, O., & Simoncelli, E. P. (2001). Natural signal statistics and sensory gain control. *Nature Neuroscience, 4,* 819–825. [PubMed] [Article]

Sengpiel, F., Baddeley, R. J., Freeman, T. C., Harrad, R., & Blakemore, C. (1998). Different mechanisms underlie three inhibitory phenomena in cat area 17. *Vision Research, 38,* 2067–2080. [PubMed]

Sengpiel, F., & Vorobyov, V. (2005). Intracortical origins of interocular suppression in the visual cortex. *Journal of Neuroscience, 25,* 6394–6400. [PubMed] [Article]

Shani, R., & Sagi, D. (2005). Eccentricity effects on lateral interactions. *Vision Research, 45,* 2009–2024. [PubMed]

Sillito, A. M., Cudeiro, J., & Murphy, P. C. (1993). Orientation sensitive elements in the corticofugal influence on centre–surround interactions in the dorsal lateral geniculate nucleus. *Experimental Brain Research, 93,* 6–16. [PubMed]

Sillito, A. M., Grieve, K. L., Jones, H. E., Cudeiro, J., & Davis, J. (1995). Visual cortical mechanisms detecting focal orientation discontinuities. *Nature, 378,* 492–496. [PubMed]

Sillito, A. M., & Jones, H. E. (1996). Context-dependent interactions and visual processing in V1. *The Journal of Physiology, 90,* 205–209. [PubMed]

Smith, M. A., Bair, W., & Movshon, J. A. (2006). Dynamics of suppression in macaque primary visual cortex. *The Journal of Neuroscience, 26,* 4826–4834. [PubMed] [Article]

Snowden, R. J., & Hammett, S. T. (1998). The effects of surround contrast on contrast thresholds, perceived contrast, and contrast discrimination. *Vision Research, 38,* 1935–1945. [PubMed]

Solomon, J. A., & Morgan, M. J. (2000). Facilitation from collinear flanks is cancelled by non-collinear flanks. *Vision Research, 40,* 279–286. [PubMed]

Solomon, J. A., Sperling, G., & Chubb, C. (1993). The lateral inhibition of perceived contrast is indifferent to on-center/off-center segregation, but specific to orientation. *Vision Research, 33,* 2671–2683. [PubMed]

Solomon, J. A., Watson, A. B., & Morgan, M. J. (1999). Transducer model produces facilitation from opposite-sign flanks. *Vision Research, 39,* 987–992. [PubMed]

Solomon, S. G., White, A. J. R., & Martin, P. R. (2002). Extraclassical receptive field properties of parvocellular, magnocellular, and Koniocellular cells in primate lateral geniculate nucleus. *The Journal of Neuroscience, 22,* 338–349. [PubMed] [Article]

Tolhurst, D. J., & Heeger, D. J. (1997). Comparison of contrast-normalization and threshold models of the responses of simple cells in cat striate cortex. *Visual Neuroscience, 14,* 293–309. [PubMed]

Tootel, R. B. H., Switkes, E., Silverman, M. S., & Hamilton, S. L. (1988). Functional anatomy of macaque striate cortex II. Retinotopic organization. *The Journal of Neuroscience, 8,* 1531–1568. [PubMed] [Article]

Watson, A. B., & Solomon, J. A. (1997). A model of visual contrast gain control and pattern masking. *Journal of the Optical Society of America, 14,* 2379–2391. [PubMed]

Webb, B. S., Dhruv, N. T., Solomon, S. G., Tailby, C., & Lennie, P. (2005). Early and late mechanisms of surround suppression in striate cortex of Macaque. *The Journal of Neuroscience, 25,* 11666–11675. [PubMed] [Article]

Webb, B. S., Tinsley, C. J., Barraclough, N. E., Easton, A., Parker, A., & Derrington, A. M. (2002). Feedback from

V1 and inhibition from beyond the classical receptive field modulates the responses of neurons in the primate lateral geniculate nucleus. *Visual Neuroscience, 19,* 583–592. [PubMed]

Webb, B. S., Tinsley, C. J., Barraclough, N. E., Parker, A., & Derrington, A. M. (2003). Gain control from beyond the classical receptive field in primate visual cortex. *Visual Neuroscience, 20,* 221–230. [PubMed]

Wetherill, G. B., & Levitt, H. (1965). Sequential estimation of points on a psychometric function. *British Journal of Mathematical & Statistical Psychology, 18,* 1–10. [PubMed]

Williams, A. L., Singh, K. D., & Smith, A. T. (2003). Surround modulation with functional MRI in the human visual cortex. *Journal of Neurophysiology, 89,* 525–533. [PubMed] [Article]

Williams, C. B., & Hess, R. F. (1998). Relationship between facilitation at threshold and suprathreshold contour integration. *Journal of the Optical Society of America A, Optics, Image Science, and Vision, 15,* 2046–2051. [PubMed]

Woods, R. L., Nugent, A. K., & Peli, N. E. (2002). Lateral interactions: Size does matter. *Vision Research, 42,* 733–745. [PubMed]

Xing, J., & Heeger, D. J. (2000). Centre–surround interactions in foveal and peripheral vision. *Vision Research, 40,* 3065–3072. [PubMed]

Xing, J., & Heeger, D. J. (2001). Measurement and modeling of center–surround suppression and enhancement. *Vision Research, 41,* 571–583. [PubMed]

Yu, C., Klein, S. A., & Levi, D. M. (2001). Surround modulation of perceived contrast and the role of brightness induction. *Journal of Vision, 1*(1):3, 18–31, http://journalofvision.org/1/1/3/, doi:10.1167/1.1.3. [PubMed] [Article]

Yu, C., Klein, S. A., & Levi, D. M. (2002). Facilitation of contrast detection by cross-oriented surround stimuli and its psychophysical mechanisms. *Journal of Vision, 2*(3):4, 243–255, http://journalofvision.org/2/3/4/, doi:10.1167/2.3.4. [PubMed] [Article]

Yu, C., Klein, S. A., & Levi, D. M. (2003). Cross- and iso-oriented surrounds modulate the contrast response function: The effect of surround contrast. *Journal of Vision, 3*(8):1, 527–540, http://journalofvision.org/3/8/1/, doi:10.1167/3.8.1. [PubMed] [Article]

Yu, C., & Levi, D. M. (2000). Surround modulation in human vision unmasked by masking experiments. *Nature Neuroscience, 3,* 724–728. [PubMed] [Article]

Zenger-Landolt, B., & Heeger, D. J. (2003). Response suppression in V1 agrees with psychophysics of surround masking. *The Journal of Neuroscience, 23,* 6884–6893. [PubMed] [Article]